

Numerical Simulation of Nonlinear Electromagnetic Wave Propagation in Nematic Liquid Crystal Cells

N.C. Papanicolaou¹ M.A. Christou¹ A.C. Polycarpou²

¹Department of Mathematics, University of Nicosia

²Department of Electrical and Computer Engineering, University of Nicosia

4th EAC for AMiTaNS, Varna, Bulgaria, June 11-16, 2012

In memory of Prof. C. I. Christov

Ack.: The work of N.C. Papanicolaou and M.A. Christou was partially supported by grant DDVU02/71, NSF, Bulgarian Ministry of Education, Youth and Science



Radio-Telecommunications Lab
RTeLab

Outline

- 1 Introduction
- 2 Formulation and Analysis
 - Description and Geometry
 - Maxwell Equations
 - Mode-Matching Technique
 - Non-Linear Equation for the Director Field
 - Finite Difference Schemes and Boundary Conditions
- 3 Results
 - Rigid Anchoring - Normal Incidence
 - Soft Anchoring - Normal Incidence
 - Rigid Anchoring - Oblique Incidence
- 4 Summary



Outline

- 1 Introduction
- 2 Formulation and Analysis
 - Description and Geometry
 - Maxwell Equations
 - Mode-Matching Technique
 - Non-Linear Equation for the Director Field
 - Finite Difference Schemes and Boundary Conditions
- 3 Results
 - Rigid Anchoring - Normal Incidence
 - Soft Anchoring - Normal Incidence
 - Rigid Anchoring - Oblique Incidence
- 4 Summary



Outline

- 1 Introduction
- 2 Formulation and Analysis
 - Description and Geometry
 - Maxwell Equations
 - Mode-Matching Technique
 - Non-Linear Equation for the Director Field
 - Finite Difference Schemes and Boundary Conditions
- 3 Results
 - Rigid Anchoring - Normal Incidence
 - Soft Anchoring - Normal Incidence
 - Rigid Anchoring - Oblique Incidence
- 4 Summary



Outline

- 1 Introduction
- 2 Formulation and Analysis
 - Description and Geometry
 - Maxwell Equations
 - Mode-Matching Technique
 - Non-Linear Equation for the Director Field
 - Finite Difference Schemes and Boundary Conditions
- 3 Results
 - Rigid Anchoring - Normal Incidence
 - Soft Anchoring - Normal Incidence
 - Rigid Anchoring - Oblique Incidence
- 4 Summary



- Liquid Crystals are of particular interest because of their use in various devices such as LCDs, optical filters and switches, beam-steering devices, LC-thermometers. This is due to their electro-optical properties (anisotropic, birefringent and tunable).
- In this presentation, we develop an efficient and robust numerical method for the simulation of Electromagnetic Wave Propagation in Liquid Crystal Cells. We concentrate on Nematic Liquid crystals.
- The cases of both normal and oblique incidence are examined and interesting phenomena such as hysteresis and bistability are presented.



- Liquid Crystals are of particular interest because of their use in various devices such as LCDs, optical filters and switches, beam-steering devices, LC-thermometers. This is due to their electro-optical properties (anisotropic, birefringent and tunable).
- In this presentation, we develop an efficient and robust numerical method for the simulation of Electromagnetic Wave Propagation in Liquid Crystal Cells. We concentrate on Nematic Liquid crystals.
- The cases of both normal and oblique incidence are examined and interesting phenomena such as hysteresis and bistability are presented.



- Liquid Crystals are of particular interest because of their use in various devices such as LCDs, optical filters and switches, beam-steering devices, LC-thermometers. This is due to their electro-optical properties (anisotropic, birefringent and tunable).
- In this presentation, we develop an efficient and robust numerical method for the simulation of Electromagnetic Wave Propagation in Liquid Crystal Cells. We concentrate on Nematic Liquid crystals.
- The cases of both normal and oblique incidence are examined and interesting phenomena such as hysteresis and bistability are presented.



Nematic Liquid Crystals

- Nematic liquid crystals owe their properties to their molecular structure. Their molecules are rod-like (calametic) and in this mesophase they macroscopically point in a preferred direction called the *director*.
- The orientation of the directors determines the electrical properties of the liquid crystal. Thus, the relative dielectric tensor of the LC is a function of the director angle.
- In the presence of an applied electric (or magnetic) field above a certain intensity the directors reorient, changing the optical properties of the liquid crystal. This is called the *Fréedericksz Transition*.



Nematic Liquid Crystals

- Nematic liquid crystals owe their properties to their molecular structure. Their molecules are rod-like (calametic) and in this mesophase they macroscopically point in a preferred direction called the *director*.
- The orientation of the directors determines the electrical properties of the liquid crystal. Thus, the relative dielectric tensor of the LC is a function of the director angle.
- In the presence of an applied electric (or magnetic) field above a certain intensity the directors reorient, changing the optical properties of the liquid crystal. This is called the *Fréedericksz Transition*.



Nematic Liquid Crystals

- Nematic liquid crystals owe their properties to their molecular structure. Their molecules are rod-like (calametic) and in this mesophase they macroscopically point in a preferred direction called the *director*.
- The orientation of the directors determines the electrical properties of the liquid crystal. Thus, the relative dielectric tensor of the LC is a function of the director angle.
- In the presence of an applied electric (or magnetic) field above a certain intensity the directors reorient, changing the optical properties of the liquid crystal. This is called the *Fréedericksz Transition*.



A Nematic Liquid Crystal Cell

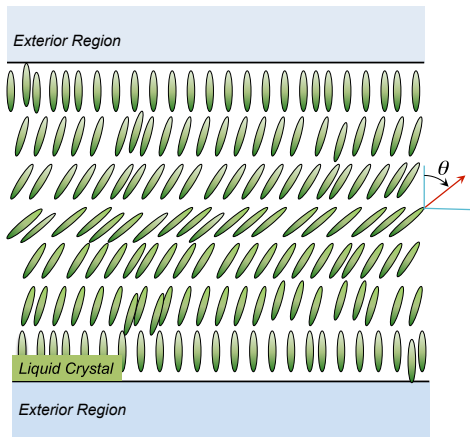


Figure: A nematic liquid crystal cell. At the boundaries rigid anchoring with homeotropic alignment is assumed.



Problem Dynamics

- Here, a uniform plane wave polarized along the plane of incidence (xz -plane) (*pump beam, usually a laser*) excites the LC, changing the orientation angle of the directors.
- This alters the dielectric tensor and hence affects the intensity of the electric and magnetic fields inside the cell. In turn, the new light intensity leads to corresponding new values for the director field.
- This a coupled problem. The set of Maxwell equations modeling the propagation of the electromagnetic wave is intrinsically linked to the Nonlinear Differential Equation for the director field.





Problem Dynamics

- Here, a uniform plane wave polarized along the plane of incidence (xz -plane) (*pump beam, usually a laser*) excites the LC, changing the orientation angle of the directors.
- This alters the dielectric tensor and hence affects the intensity of the electric and magnetic fields inside the cell. In turn, the new light intensity leads to corresponding new values for the director field.
- This a coupled problem. The set of Maxwell equations modeling the propagation of the electromagnetic wave is intrinsically linked to the Nonlinear Differential Equation for the director field.





Problem Dynamics

- Here, a uniform plane wave polarized along the plane of incidence (xz -plane) (*pump beam, usually a laser*) excites the LC, changing the orientation angle of the directors.
- This alters the dielectric tensor and hence affects the intensity of the electric and magnetic fields inside the cell. In turn, the new light intensity leads to corresponding new values for the director field.
- This a coupled problem. The set of Maxwell equations modeling the propagation of the electromagnetic wave is intrinsically linked to the Nonlinear Differential Equation for the director field.



Geometry

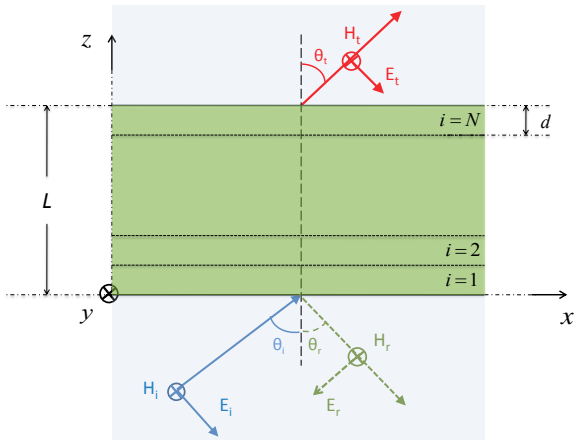


Figure: Propagation of an EM-wave that is obliquely incident to a nematic LC-cell. Regions 1, 2 and 3: Before, inside and after the LC-cell respectively.



EM-wave propagation inside the cell is modeled by the *time-harmonic Maxwell Equations*

$$\nabla \times \mathbf{E} = -j\omega\mu_0\mathbf{H}, \quad (1a)$$

$$\nabla \times \mathbf{H} = j\omega\epsilon_0\hat{\epsilon}\mathbf{E}, \quad (1b)$$

\mathbf{E} : electric field intensity

\mathbf{H} : magnetic field intensity

ϵ_0 : electric permittivity of free space

μ_0 : magnetic permeability of free space

η_0 : intrinsic impedance of vacuum ($\eta_0 = \sqrt{\mu_0/\epsilon_0}$)

$\hat{\epsilon}$ is the *LC relative permittivity tensor*, with components



$$\hat{\epsilon}(z) = \begin{bmatrix} \epsilon_{xx}(z) & 0 & \epsilon_{xz}(z) \\ 0 & \epsilon_{yy}(z) & 0 \\ \epsilon_{zx}(z) & 0 & \epsilon_{zz}(z) \end{bmatrix}, \quad (2a)$$

and

$$\begin{aligned} \epsilon_{xx} &= n_e^2 \sin^2 \theta(z) + n_o^2 \cos^2 \theta(z), \\ \epsilon_{xz} &= \epsilon_{zx} = (n_e^2 - n_o^2) \sin \theta(z) \cos \theta(z), \\ \epsilon_{yy} &= n_o^2, \\ \epsilon_{zz} &= n_e^2 \cos^2 \theta(z) + n_o^2 \sin^2 \theta(z). \end{aligned} \quad (2b)$$

n_o : the ordinary refractive index (wave polarized perpendicular to the directors)

n_e : the extraordinary refractive index (wave polarized parallel to the directors)



Because the incident wave is propagating in the xz -plane, the field components are independent of the y coordinate, i.e.,

$$\frac{\partial F}{\partial y} = 0 \quad \text{where } F = E_x, E_y, E_z, H_x, H_y \text{ or } H_z.$$

Thus, Eqs. (1,2) in component form read:

$$\frac{\partial E_y}{\partial z} = j\omega\mu_0 H_x, \quad \frac{\partial H_y}{\partial z} = -j\omega\epsilon_0[\epsilon_{xx}E_x + \epsilon_{xz}E_z], \quad (3a)$$

$$\frac{\partial E_x}{\partial z} = \frac{\partial E_z}{\partial x} - j\omega\mu_0 H_y, \quad \frac{\partial H_x}{\partial z} = \frac{\partial H_z}{\partial x} + j\omega\epsilon_0\epsilon_{yy}E_y, \quad (3b)$$

$$\frac{\partial E_y}{\partial x} = -j\omega\mu_0 H_z, \quad \frac{\partial H_y}{\partial x} = j\omega\epsilon_0[\epsilon_{zx}E_x + \epsilon_{zz}E_z]. \quad (3c)$$



Region 1

Incident electric and magnetic fields:

$$\mathbf{E}_i = (\mathbf{a}_x \cos \theta_i - \mathbf{a}_z \sin \theta_i) E_0 e^{-j(\mathbf{k}_i \cdot \mathbf{r})}, \quad (4a)$$

$$\mathbf{H}_i = \frac{n_s}{\eta_0} (\mathbf{a}_{k_i} \times \mathbf{E}_i), \quad (4b)$$

- $\mathbf{k}_i = \mathbf{a}_{k_i} k_0 n_s$: wave vector
 $k_0 = \omega \sqrt{\mu_0 \epsilon_0}$: wavenumber in vacuum
 $\mathbf{a}_{k_i} = \mathbf{a}_x \sin \theta_i + \mathbf{a}_z \cos \theta_i$: unit vector in direction of propagation
 n_s : refractive index of exterior region
 $\mathbf{r} = \mathbf{a}_x X + \mathbf{a}_z Z$: position vector of observation point in xz-plane

Therefore,

$$\mathbf{E}_i = (\mathbf{a}_x \cos \theta_i - \mathbf{a}_z \sin \theta_i) E_0 e^{-jk_0 n_s (x \sin \theta_i + z \cos \theta_i)}, \quad (5a)$$

$$\mathbf{H}_i = \mathbf{a}_y \frac{n_s E_0}{\eta_0} e^{-jk_0 n_s (x \sin \theta_i + z \cos \theta_i)}. \quad (5b)$$



Region 1 (continued)

Snell's law of reflection implies $\theta_r = \theta_i$. Hence, the reflected wave propagates in the direction of the unit vector $\mathbf{a}_{k_r} = \mathbf{a}_x \sin \theta_i - \mathbf{a}_z \cos \theta_i$.

Therefore,

$$\mathbf{E}_r = (-\mathbf{a}_x \cos \theta_i - \mathbf{a}_z \sin \theta_i) \Gamma E_0 e^{-jk_0 n_s (x \sin \theta_i - z \cos \theta_i)}, \quad (6a)$$

$$\mathbf{H}_r = \frac{n_s}{\eta_0} \mathbf{a}_{k_r} \times \mathbf{E}_r = \mathbf{a}_y \frac{n_s \Gamma E_0}{\eta_0} e^{-jk_0 n_s (x \sin \theta_i - z \cos \theta_i)}, \quad (6b)$$

where Γ is the reflection coefficient in the plane of incidence.

Consequently, in the lower exterior region, the total field is simply the superposition of the incident and reflected fields

$$\mathbf{E} = \mathbf{E}_i + \mathbf{E}_r = (\mathbf{a}_x \cos \theta_i - \mathbf{a}_z \sin \theta_i) E_0 e^{-jk_0 n_s (x \sin \theta_i + z \cos \theta_i)} - (\mathbf{a}_x \cos \theta_i + \mathbf{a}_z \sin \theta_i) \Gamma E_0 e^{-jk_0 n_s (x \sin \theta_i - z \cos \theta_i)}, \quad (7a)$$

$$\mathbf{H} = \mathbf{H}_i + \mathbf{H}_r = \mathbf{a}_y \frac{n_s E_0}{\eta_0} e^{-jk_0 n_s (x \sin \theta_i + z \cos \theta_i)} + \mathbf{a}_y \frac{\Gamma n_s E_0}{\eta_0} e^{-jk_0 n_s (x \sin \theta_i - z \cos \theta_i)}. \quad (7b)$$

Region 3

Similarly, the transmitted fields in the upper region are given by

$$\mathbf{E}_t = (\mathbf{a}_x \cos \theta_t - \mathbf{a}_z \sin \theta_t) TE_0 e^{-jk_0 n_s (x \sin \theta_t + z \cos \theta_t)}, \quad (8a)$$

$$\mathbf{H}_t = \mathbf{a}_y \frac{n_s TE_0}{\eta_0} e^{-jk_0 n_s (x \sin \theta_t + z \cos \theta_t)} \quad (8b)$$

where $\theta_t = \theta_i$ and T is the copolarized transmission coefficient at the upper interface, which separates the crystal and the exterior region.



Region 2

To satisfy continuity of the tangential fields for all x at a fixed z -plane, the fields inside the LC-cell are written:

$$\mathbf{E}(z, x) = \mathbf{E}(z) e^{-jk_0 n_s x \sin \theta_i} \quad \text{and} \quad \mathbf{H}(z, x) = \mathbf{H}(z) e^{-jk_0 n_s x \sin \theta_i} . \quad (9)$$

So, the field components are of the form

$$F(x, z) = F(z) e^{-j k_0 n_s x \sin \theta_i} \quad (10)$$

where $F = E_x, E_y, E_z, H_x, H_y$ or H_z .

Clearly,

$$\frac{\partial F(x, z)}{\partial x} = -jk_0 S F(x, z), \quad (11)$$

where $S = n_s \sin \theta_i$. Substituting (11) into (3), employing (10) and manipulating yields:



$$\frac{\partial u_1}{\partial z} = j k_0 [c_{11} u_1 + c_{14} u_4], \quad \frac{\partial u_2}{\partial z} = j k_0 u_3, \quad (12a)$$

$$\frac{\partial u_3}{\partial z} = j k_0 c_{32} u_2, \quad \frac{\partial u_4}{\partial z} = j k_0 [c_{41} u_1 + c_{44} u_4]. \quad (12b)$$

where

$$u_1 = E_x, \quad u_2 = E_y, \quad u_3 = \eta_0 H_x, \quad u_4 = \eta_0 H_y,$$

$$c_{11} = (\epsilon_{zx}/\epsilon_{zz})S, \quad c_{14} = (S^2/\epsilon_{zz}) - 1, \quad c_{32} = \epsilon_{yy} - S^2,$$

$$c_{41} = (\epsilon_{xz}\epsilon_{zx}/\epsilon_{zz}) - \epsilon_{xx}, \quad c_{44} = S(\epsilon_{xz}/\epsilon_{zz}).$$

- The LC cell is then subdivided into N layers of thickness d . Each of these layers is assumed to be homogeneous and anisotropic. The dielectric properties of the layer are characterized by $\hat{\epsilon}$ in Eq. (2a) and thus depend on the director field θ evaluated at the midpoint of the layer.
- The solutions of Eqs. (12) have the following generic form:

$$u_m(z) \propto e^{-jk_0 n z}, \quad (13)$$

where $m = 1, 2, 3, 4$ and n is the unknown refractive index inside the homogeneous LC layer.

- Substituting Eq. (13) into Eqs. (12) results in the following system of algebraic equations:

$$(n + c_{11})u_1 + c_{14}u_4 = 0, \quad (14a)$$

$$nu_2 + u_3 = 0, \quad (14b)$$

$$c_{32}u_2 + nu_3 = 0, \quad (14c)$$

$$c_{41}u_1 + (n + c_{44})u_4 = 0. \quad (14d)$$

- For the homogeneous system (14) to have a nontrivial solution, $\det(A) = 0$, which leads to the following algebraic equation for n

$$(n^2 - c_{32}) [(n + c_{11})(n + c_{44}) - c_{41}c_{14}] = 0, \quad (15)$$

which admits solutions

$$n_{1,2} = \pm\sqrt{c_{32}}, \quad n_{3,4} = -c_{11} \pm \sqrt{c_{14}c_{41}}. \quad (16)$$

- *Eqs. (14a, 14d) and solutions $n_{3,4}$ correspond to an incident plane wave polarized in a direction parallel to the plane of incidence.*
- Eqs. (14b, 14c) and solutions $n_{1,2}$ correspond to an incident plane wave polarized in a direction perpendicular to the plane of incidence.

Region 2 (continued)

- Because $\epsilon_{xy} = \epsilon_{yx} = \epsilon_{yz} = \epsilon_{zy} = 0$, the two polarizations are fully decoupled (see Eqs. 14).
- This means that an incident plane wave polarized in a direction perpendicular to the plane of incidence will not generate field components inside the LC that are polarized in the parallel direction and vice-versa.
- *To trigger the formation of an extraordinary wave inside the LC cell, the incident plane wave must be polarized in a direction parallel to the plane of incidence.* Therefore:

$$u_1(z) = A e^{-j k_0 n_3 z} + B e^{-j k_0 n_4 z}, \quad (17a)$$

$$u_4(z) = - \left(\frac{c_{41}}{n_3 + c_{44}} \right) A e^{-j k_0 n_3 z} - \left(\frac{c_{41}}{n_4 + c_{44}} \right) B e^{-j k_0 n_4 z}, \quad (17b)$$

where n_3 and n_4 are given by Eqs. (16). Note also that

$$u_1(x, z) = u_1(z) e^{-j k_0 x \sin \theta_i}, \quad (18a)$$

$$u_4(x, z) = u_4(z) e^{-j k_0 x \sin \theta_i}. \quad (18b)$$

Mode-Matching

- The unknown coefficients are obtained by enforcing the continuity of the tangential fields at the interfaces. As mentioned earlier, the LC is subdivided into N equally thin homogeneous layers.
- The first interface is between the lower exterior region (Region 1) and the first layer of the LC and the last interface is between the last LC-layer and Region 3. The total number of interfaces is equal to $N + 1$. This leads to $2N + 2$ linear equations with $2N + 2$ unknowns.
- Two of these correspond to the reflection and transmission coefficients in the plane of incidence. The remaining unknowns correspond to the modal expansion coefficients representing the fields inside the LC.



Lower Exterior Region:

$$u_1(z) = E_0 \cos \theta_i e^{-jn_s k_0 z \cos \theta_i} - \Gamma E_0 \cos \theta_i e^{jn_s k_0 z \cos \theta_i}, \quad (19a)$$

$$u_4(z) = n_s E_0 e^{-jn_s k_0 z \cos \theta_i} + n_s \Gamma E_0 e^{jn_s k_0 z \cos \theta_i}. \quad (19b)$$

LC Region:

$$u_{1,m}(z) = A_m e^{-j k_0 n_3 (z-d_m)} + B_m e^{-j k_0 n_4 (z-d_m)}, \quad (20a)$$

$$u_{4,m}(z) = -C_A A_m e^{-j k_0 n_3 (z-d_m)} - C_B B_m e^{-j k_0 n_4 (z-d_m)}, \quad (20b)$$

where $C_A = c_{41} / (n_3 + c_{44})$, $C_B = c_{41} / (n_4 + c_{44})$, and $d_m = (m - 1)d$; $m = 1, 2, \dots, N$, where the index m indicates the layer number.

Upper Exterior Region:

$$u_1(z) = TE_0 \cos \theta_i e^{-jn_s k_0 (z-d_{N+1}) \cos \theta_i}, \quad (21a)$$

$$u_4(z) = n_s TE_0 e^{-jn_s k_0 (z-d_{N+1}) \cos \theta_i}. \quad (21b)$$

Note: The z coordinate was transformed to $z - z_0$, where z_0 corresponds to the z coordinate of the lower layer interface.



Enforcing the continuity of u_1 and u_4 at each of the $N + 1$ interfaces yields

$$\begin{aligned} z = 0 & & : & \quad \Gamma E_0 \cos \theta_i + A_1 + B_1 = E_0 \cos \theta_i, \\ & & : & \quad -n_s \Gamma E_0 - C_A A_1 - C_B B_1 = n_s E_0, \end{aligned}$$

$$\begin{aligned} z = d & & : & \quad A_1 e^{-j k_0 n_3 d} + B_1 e^{-j k_0 n_4 d} - A_2 - B_2 = 0, \\ & & & \quad A_1 C_A e^{-j k_0 n_3 d} + B_1 C_B e^{-j k_0 n_4 d} - A_2 C_A - B_2 C_B = 0, \end{aligned}$$

$$\vdots$$

$$\begin{aligned} z = (m-1)d & & : & \quad A_{m-1} e^{-j k_0 n_3 d} + B_{m-1} e^{-j k_0 n_4 d} - A_m - B_m = 0, \\ & & & \quad A_{m-1} C_A e^{-j k_0 n_3 d} + B_{m-1} C_B e^{-j k_0 n_4 d} - A_m C_A - B_m C_B = 0, \end{aligned}$$

$$\vdots$$

$$\begin{aligned} z = Nd & & : & \quad A_N e^{-j k_0 n_3 d} + B_N e^{-j k_0 n_4 d} - E_0 \cos \theta_i T = 0, \\ & & : & \quad C_A A_N e^{-j k_0 n_3 d} + C_B B_N e^{-j k_0 n_4 d} - n_s E_0 \cos \theta_i T = 0. \end{aligned}$$

The above system is solved using LU decomposition to obtain the expansion coefficients and the reflection and transmission coefficients at the lower and upper interfaces, respectively.



Non-Linear ODE for the Director Field

The orientation of the directors inside a LC in the presence of an electromagnetic field is governed by the following functional which represents the total free energy per unit volume:

$$\mathcal{F} = \int \left[\frac{1}{2} k_{11} (\nabla \cdot \hat{n})^2 + \frac{1}{2} k_{22} [\hat{n} \cdot (\nabla \times \hat{n})]^2 + \frac{1}{2} k_{33} \|\hat{n} \times (\nabla \times \hat{n})\|^2 - \frac{l}{c} \tilde{n}(\theta) \right] d^3 r, \quad (22)$$

where

$$\tilde{n} = \frac{n_o n_e}{\sqrt{n_o^2 \sin^2 \theta + n_e^2 \cos^2 \theta}} \quad \text{and} \quad \hat{n} = (\sin \theta, 0, \cos \theta), \quad (23)$$

c the speed of light in a vacuum, $l = \frac{1}{2} \Re[(\mathbf{E} \times \mathbf{H}^*) \cdot \mathbf{a}_z] = \frac{1}{2} \Re[E_x H_y^*]$ the local light intensity, and k_{11} , k_{22} and k_{33} are the splay, twist and bend elastic constants.

Functional \mathcal{F} attains its minimal value when the Euler-Lagrange equation

$$\frac{\partial f}{\partial \theta} - \frac{d}{dz} \frac{\partial f}{\partial \theta_z} = 0 \quad (24)$$

holds, where f is the integrand in Eqn. (22)



Substituting Eqn. (23) into the integrand of (22) yields

$$f = \frac{1}{2}k_{11}\theta_z^2 \sin^2 \theta + \frac{1}{2}k_{33}\theta_z^2 \cos^2 \theta - \frac{l}{c} \frac{n_0 n_e}{\sqrt{n_0^2 \sin^2 \theta + n_e^2 \cos^2 \theta}}. \quad (25)$$

Replacing (25) into the Euler-Lagrange equation and rearranging leads to the nonlinear ODE for the directors

$$\theta_{zz} - \frac{k \sin 2\theta}{2(1 - k \sin^2 \theta)} \theta_z^2 + \frac{\alpha(z) \sin 2\theta}{(1 - k \sin^2 \theta)(1 - \beta \sin^2 \theta)^{3/2}} = 0, \quad (26)$$

where $k = (k_{33} - k_{11})/k_{33}$, $\beta = 1 - (n_0/n_e)^2$ and $\alpha(z) = \frac{\beta n_0 l(z)}{2ck_{33}}$. Utilizing the definition of the Fréedericksz threshold intensity, I_{Fr} ,

$$I_{Fr} = \frac{ck_{33}\pi^2}{n_0\beta L^2} \quad (27)$$

(26) can be expressed as

$$\theta_{zz} - \frac{1}{2} \frac{k \sin 2\theta}{(1 - k \sin^2 \theta)} \theta_z^2 + \frac{1}{2} \left(\frac{\pi}{L}\right)^2 \frac{l}{I_{Fr}} \frac{\sin 2\theta}{(1 - k \sin^2 \theta)(1 - \beta \sin^2 \theta)^{3/2}} = 0. \quad (28)$$

Boundary Conditions

- The orientation of the directors versus the z coordinate is posed as a two-point boundary value problem, governed by (28), and a set of boundary conditions at the walls of the cell.
- For strong anchoring, the two boundary conditions are of Dirichlet type:

$$\theta(z = 0) = 0 \quad \text{and} \quad \theta(z = L) = 0. \quad (29)$$

- For soft anchoring, the boundary conditions are of Robin type expressed as first-order differential equations:

$$k_{33}(1 - k \sin^2 \theta) \left(\frac{d\theta}{dz} \right) + \frac{1}{2} \left(\frac{dF}{dz} \right) = 0 \quad \text{at} \quad z = 0, L, \quad (30)$$

where $F(\theta) = C \cos^2 \theta + C_4 \cos^4 \theta$ is known as the interfacial potential.



Finite Difference Schemes

- 3-point explicit scheme:

$$\begin{aligned}\theta_i^{k+1} &= \frac{1}{3} \left[\theta_{i+1}^k + \theta_i^k + \theta_{i-1}^k - \frac{k \sin 2\theta_i^k (\theta_{i+1}^k - \theta_{i-1}^k)^2}{8(1 - k \sin^2 \theta_i^k)} \right] \\ &+ \frac{1}{6} \left(\frac{\pi}{L} \right)^2 \frac{l}{l_{Fr}} \frac{h^2 \sin 2\theta_i^k}{(1 - k \sin^2 \theta_i^k)(1 - \beta \sin^2 \theta_i^k)^{3/2}}.\end{aligned}\quad (31)$$

- 5-point explicit scheme:

$$\begin{aligned}\theta_i^{k+1} &= \frac{1}{8} \left[\theta_{i+2}^k + \theta_{i+1}^k + 4\theta_i^k + \theta_{i-1}^k + \theta_{i-2}^k \right] \\ &- \frac{5k \sin 2\theta_i^k}{64(1 - k \sin^2 \theta_i^k)} (\theta_{i+1}^k - \theta_{i-1}^k)^2 \\ &+ \frac{5h^2}{16} \left(\frac{\pi}{L} \right)^2 \frac{l}{l_{Fr}} \frac{\sin 2\theta_i^k}{(1 - k \sin^2 \theta_i^k)(1 - \beta \sin^2 \theta_i^k)^{3/2}}.\end{aligned}\quad (32)$$

Derivation:

$$\theta'' = \frac{\theta_{i+2} + \theta_{i+1} - 4\theta_i + \theta_{i-1} + \theta_{i-2}}{5h^2} + O(h^2).\quad (33)$$

- 3-point semi-implicit scheme:

$$(1 - \omega_1) (\theta_{i+1}^{m+1} - 2\theta_i^{m+1} + \theta_{i-1}^{m+1}) + \omega_1 (\theta_{i+1}^m - 2\theta_i^m + \theta_{i-1}^m) - \frac{k \sin 2\theta_i^m}{8(1 - k \sin^2 \theta_i^m)} \left[(1 - \omega_2) (\theta_{i+1}^m - \theta_{i-1}^m) (\theta_{i+1}^{m+1} - \theta_{i-1}^{m+1}) + \omega_2 (\theta_{i+1}^m - \theta_{i-1}^m)^2 \right] + \frac{1}{2} \left(\frac{\pi}{L} \right)^2 \frac{l}{I_{Fr}} \frac{h^2 \sin 2\theta_i^m}{(1 - k \sin^2 \theta_i^m) (1 - \beta \sin^2 \theta_i^m)^{3/2}} = 0, \quad (34)$$

where ω_1, ω_2 are the relaxation parameters for the second and first derivatives, respectively.

- Note: The 5-point scheme reverts to a 3-point scheme near the boundaries.
- The Robin type boundary conditions for soft anchoring, (30) are discretized as follows:

$$\theta_i^{k+1} = \theta_{i+1}^k - \frac{h \sin \theta_i (C \cos \theta_i + 2C_4 \cos^3 \theta_i)}{k_{33}(1 - k \sin^2 \theta_i)}, \quad \text{at } z = 0, \quad (35a)$$

$$\theta_i^{k+1} = \theta_{i-1}^k - \frac{h \sin \theta_i (C \cos \theta_i + 2C_4 \cos^3 \theta_i)}{k_{33}(1 - k \sin^2 \theta_i)}, \quad \text{at } z = L. \quad (35b)$$



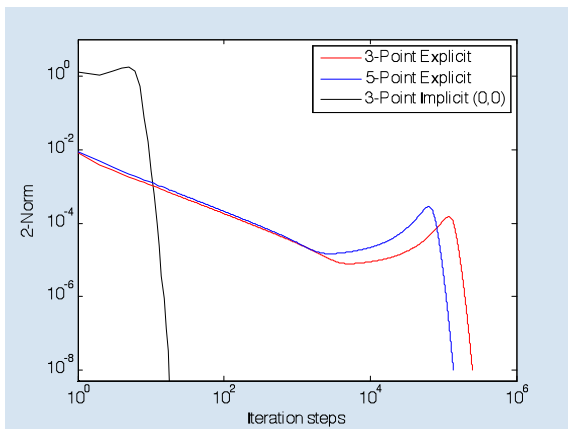


Figure: Comparison of the convergence rates of the proposed finite difference schemes for Methoxybenzylidene butylaniline (MBBA) and homeotropic alignment.

$\theta = \theta(z)$ for $\theta_i = 0$ and homeotropic b.c.s

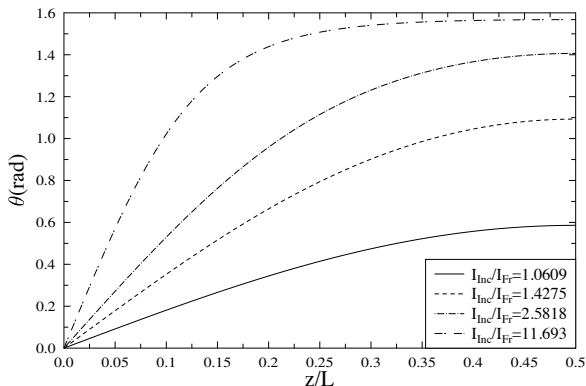


Figure: The directors' tilt angle as a function of space ($0 \leq z \leq L/2$) for four different biased intensities.



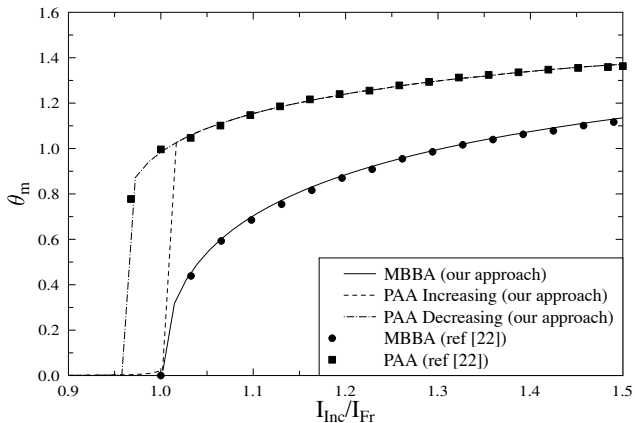


Figure: θ_{max} vs scaled incident intensity for MBBA ($\lambda = 632.8$ nm, $n_o = 1.544$, $n_e = 1.758$, $k_{11} = 6.95 \times 10^{-12}$ N, $k_{33} = 8.99 \times 10^{-12}$ N) and PAA ($\lambda = 480$ nm, $n_o = 1.595$, $n_e = 1.995$, $k_{11} = 9.26 \times 10^{-12}$ N, $k_{33} = 18.1 \times 10^{-12}$ N). For both cases, the refractive index of the exterior region $n_s = n_o$. For MBBA $B = 0.25(1 - k - 2.25\beta) > 0$, whereas for PAA $B < 0$.

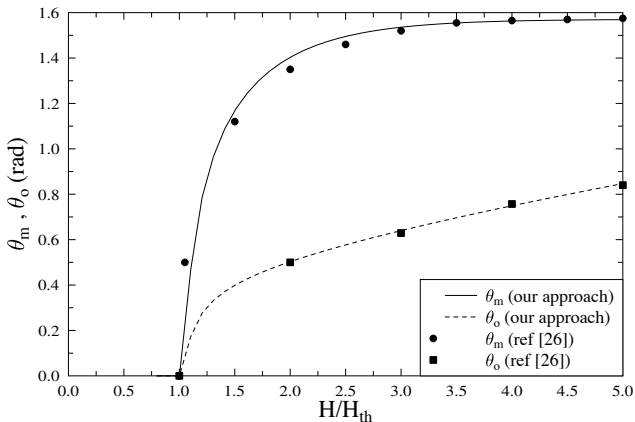


Figure: Maximum director angle (θ_m) and interfacial director angle (θ_o) versus the normalized applied magnetic field. MBBA liquid crystal cell at a temperature $T = 39.5^\circ$ having the following specifications: $L = 2.9\mu\text{m}$, $\lambda = 632.8\text{ nm}$, $n_o = 1.5507$, $n_e = 1.7352$, $k_{11} = 5.3 \times 10^{-12}\text{ N}$, $k_{33} = 5.7 \times 10^{-12}\text{ N}$. The exterior region is glass. Soft anchoring is applied at the liquid crystal-to-wall interface with an interfacial potential $F(\theta) = 47.0\cos^2\theta - 18.0\cos^4\theta\ \mu\text{N/m}$.



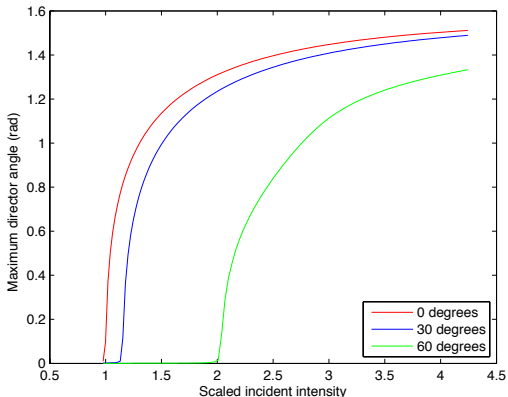


Figure: Maximum director angle θ_m as a function of the scaled incident intensity I_{inc}/I_{Fr} for MBBA at different angles of incidence.



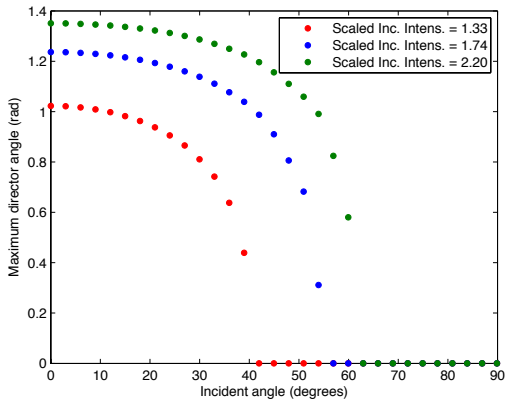


Figure: Maximum director angle θ_m as a function of the incident angle for MBBA at different values of the scaled incident intensity I_{inc}/I_{Fr} .



Summary

- A numerical method is presented for treating electromagnetic wave propagation in Nematic Liquid Crystal cells. The problem is governed by the Maxwell time-harmonic equations coupled with a nonlinear ODE for the tilt angle of the directors.
- These are solved iteratively; the Mode-Matching Technique is used for the Maxwell equations and a semi-implicit Finite Difference scheme is employed for the ODE governing the director field.
- The proposed method was validated by comparing the obtained results for some indicative parameter values with published data and were found to be in very good agreement.
- Finally, the method is used to treat a variety of cases revealing including finite anchoring and oblique incidence.

Summary

- A numerical method is presented for treating electromagnetic wave propagation in Nematic Liquid Crystal cells. The problem is governed by the Maxwell time-harmonic equations coupled with a nonlinear ODE for the tilt angle of the directors.
- These are solved iteratively; the Mode-Matching Technique is used for the Maxwell equations and a semi-implicit Finite Difference scheme is employed for the ODE governing the director field.
- The proposed method was validated by comparing the obtained results for some indicative parameter values with published data and were found to be in very good agreement.
- Finally, the method is used to treat a variety of cases revealing including finite anchoring and oblique incidence.

Summary

- A numerical method is presented for treating electromagnetic wave propagation in Nematic Liquid Crystal cells. The problem is governed by the Maxwell time-harmonic equations coupled with a nonlinear ODE for the tilt angle of the directors.
- These are solved iteratively; the Mode-Matching Technique is used for the Maxwell equations and a semi-implicit Finite Difference scheme is employed for the ODE governing the director field.
- The proposed method was validated by comparing the obtained results for some indicative parameter values with published data and were found to be in very good agreement.
- Finally, the method is used to treat a variety of cases revealing including finite anchoring and oblique incidence.

Summary

- A numerical method is presented for treating electromagnetic wave propagation in Nematic Liquid Crystal cells. The problem is governed by the Maxwell time-harmonic equations coupled with a nonlinear ODE for the tilt angle of the directors.
- These are solved iteratively; the Mode-Matching Technique is used for the Maxwell equations and a semi-implicit Finite Difference scheme is employed for the ODE governing the director field.
- The proposed method was validated by comparing the obtained results for some indicative parameter values with published data and were found to be in very good agreement.
- Finally, the method is used to treat a variety of cases revealing including finite anchoring and oblique incidence.

For Further Reading I



P. de Gennes and J. Prost.
The Physics of Liquid Crystals.
2nd ed, Oxford: Clarendon Press, 1995.



H. L. Ong.
Optically induced Fréedericksz transition and bistability in a
nematic liquid crystal.
Phys. Rev. A, 28(4):2393–2407, 1983.



V. Ilyina, S. J. Cox, and T. J. Sluckin.
A computational approach to the optical Fréedericksz transition.
Optics Communications, 260:474–480, 2006.



K. H. Yang and C. Rosenblatt.
Determination of the anisotropic potential at the nematic liquid crystal-to-wall
interface.
Appl. Phys. Lett., 43(1):62–64, July 1983.